Water Quality Assessment with Thermal Images

Naima Khan, Nirmalya Roy
Department of Information Systems, University of Maryland, Baltimore County
nkhan4@umbc.edu, nroy@umbc.edu

***Abstract*—Water contamination has been a critical issue in many countries of the world including USA. Physical, chemical, biological, radio-logical substances can be the reason of this contamination. Drinking water systems are allowed to contain chlorine, calcium, lead, arsenic etc., at a certain level. However, there are expensive instruments and paper sensors to detect the quantity of minerals in water. But these instruments are not always convenient for easy determination of the quality of the sample as drinking water. Different minerals in the water reacts to heat heterogeneously. Some minerals (i.e., arsenic) stay in the water with noticeable amount even after reaching to boiling point. However, it requires cheaper and easier process to examine the quality of water samples for drinking from different sources. With this in mind, we experimented few water samples from different places of USA including artificially prepared samples by mixing different impurities. We investigated their heating property with the sample of marked safe drinking water. We collected thermal images with 10-seconds interval during cooling period of hot water samples from the boiling point to room temperature. We extracted features for each of the water samples with the combination of convolution and recurrent neural network based model and classified different water samples based on the added impurity types and sources from where the samples were collected. We also showed the feature distances of these water samples with the safe water sample. Our proposed framework can differentiate features for different impurities added in the water samples and detect different category of impurities with average accuracy of 70% .**

I. Introduction

Drinking water is expected to contain reasonable amount of contaminants. Any physical, chemical, biological, or radiological substances or matter in water is considered as contaminants according to Safe Drinking Water Act (SDWA) [10]. Physical contaminants such as sediment or organic material changes the physical appearance or properties of water. Different types of bacteria, viruses, protozoan, parasites are considered as biological contaminants. Chemical contaminants refers to nitrogen, lead, metals, toxic elements or compounds which might occur naturally or artificially by human. Radiological contaminants i.e. cesium, plutonium, uranium etc. creates an ionizing radiation from unbalanced protons and neutrons. However, consuming some contaminants i.e. lead, arsenic, perfluorooctanoic acid etc. above a certain level can affect human health significantly. Environmental Protection Agency (EPA) has announced a standard amount of different contaminants that can be present in drinking water which is not harmful for human health.

The contamination of drinking water has been widespread throughout the world including USA. Aged infrastructure, impaired source water, strained community finances etc. have made supplying safe drinking water a challenge in USA. In 2014, water crisis in Flint city of Michigan state created the most shocking incident in USA. In an evaluation of health-related violations of SDWA, from 1982 to 2015 around 45 million people are getting drinking water from EPA standard violated source [12]. Spatial and temporal pattern identified in this study showed violation incidence is substantially higher in rural areas than in urban areas. Besides, several states in the southwest region are struggling with recurring issues. A report from the U.S Public Interest Rights Group graded water systems of each state and mentioned 21 states which are currently failing to provide safe drinking water in schools [13]. The most common lead contamination is happened from the lead in water delivery systems i.e. water fountains, faucets, pipes etc. However, lead is not the only contaminants threatening the supply of safe drinking water in USA. According to a report from Environmental Working group, around 110 million people are exposed to the water contamination caused by per- and polyfluoroalkyl substances (PFAS) [14].

There are sensors which can provide various water properties (i.e., turbidity, pH etc.) and also detect different impurities in water. These sensors can be of various types depending on the categories of impurities. For example, turbidimeter grades the transparency of the water sample. There are different sensors to detect carbon and nitrogen content, biochemical oxygen demand (BOD), countless number of salt contents, and others. Beside of these sensors, there are also online water quality monitoring systems which worked as a reliable indicator of real time contamination events. However, collecting information about baseline water level quality, considering contextual threshold selection as well as managing operational and maintenance costs for online water quality monitoring systems made it infeasible for regular water quality assessment. Besides, there are also several chemical tester for this purpose. However, there exists lack of researches on the water assessment using smart computing.

High-resolution handheld thermal cameras are being used by geological scientists for groundwater or surface-water interaction studies and other investigations [7]. Thermal cameras helps to locate and characterize thermal anomalies in streams, lakes, and adjacent structures. Temperature variations can be used to determine the heat carried by flowing water. Interesting thermal properties of water i.e., high thermal inertia, low thermal conductivity as well as high thermal capacity approves the use of water temperature for different research purposes. A thermometer can be used to measure water temperature by immersing it into water which involves direct contact. Besides, indirect measurement of radiation emitted from the water surface can provide the radiant temperature of water using remote sensing. The spectral distribution of radiant energy consists of both the water body temperature and water surface emissivity. The emissivity of water surface and black body are approximately similar. However, the emissivity of water varies with the amount of dissolved minerals in it. Therefore, to characterize the impurities in water samples, emissivity can be chosen. Thermal imaging sensor can create a composite image which provides accurate measure of heat emitting from water surface. We selected FLIROne thermal camera which provides both RGB image and temperature image. Besides, FLIROne provide open source template for developing customized image capturing smart device application.

We attempted to capture thermal properties of water samples using thermal images from its boiling temperature to room temperature. We extracted spatio-temporal features from consecutive thermal images of water samples using ConvLSTM based deep neural network. Sequential adoption of convolution and LSTM models usually learn spatial and temporal features sub-sequentially. However, ConvLSTM can provide the opportunity of learning temporal and spatial features simultaneously and estimate how data changes between time steps. ConvLSTM has been used to extract spatiotemporal features of weather radar maps [16] and videos [17], [18]. We used ConvLSTM with sequential thermal images for water quality assessment for this study.

We artificially prepared water samples by mixing different impurities i.e., salt, pencil lead powder, fluoride etc. along with the neutral water samples for this study. We proposed a framework for measuring the water quality with thermal images using smart computing. Consecutive thermal images express the thermal properties of water which varies according to different facts i.e., turbidity, pH, hardness, minerals as well as impurities added to the water sample. Our contribution in this paper is as follows:

- We introduced a model based on ConvLSTM to extract features from consecutive thermal images for classification problem. We extracted features from temporal thermal image sequences and classified the water samples according to the materials we mixed. We also showed the similarity and dissimilarity among different water sources using the features from water samples.
- We scored each water sample by comparing their feature distance from the fresh water sample. The higher distance refers to more impurity in the water sample for drinking.

The rest of the paper is organized as follows: section II presents the relevant works in water impurity detection, section III presents the overall framework, section IV describes our proposed framework in detail, section V presents the results using our framework, VI discusses the shortcomings and future direction of our work, and VII concludes the paper.

II. Related Works

A limited amount of research in detecting water contaminants were performed in recent years. In 2006, micro-organism oocysts were identified in drinking water using simple image processing algorithms by Fernandez-Canque et.al [2]. Later in 2014, a capacitive sensor is designed using low cost parallel plate for detecting impurities such as salt, sugar, ferrous sulphate and copper sulphate [3]. Another recent research in [9] was done with 9 samples of water using chemical characteristics such as ion concentration, nutrient concentration, stream metabolism etc., of the water samples as features. They distinguished the water samples using different types of machine learning algorithms. However, these chemical properties of water samples are not often convenient to measure for easy assessment. Our project attempts to measure the water quality in perspective of safe and non-safe. Recently, University of Michigan conducted a research with Flint water crisis [8] which identified the factors involved with elevated lead in the water sources by studying lead test results along with demographic data of the water contaminated homes at city scale. Another interesting experiment was performed by adding different impurities such as sand, salt, black peepers etc. with water samples [1]. These samples were identified from visual images by extracting features using convolutional neural network. However, it would be difficult to determine the impurity types which does not change the usual appearance of water. In this experiment, all of the water samples were prepared by mixing sand which obviously change the visual appearance of water.

We used thermal images instead of RGB images for detecting the categories of impurities. A good number of qualitative research has been performed with thermal images to analyze the zone of interest for different domain specific problems. Based on the domain specific knowledge, thermal images have been observed to characterize or evaluate the concept of the zone of interest. For example, spatial pattern of land surface temperature has been quantified from the thermal images of land surfaces by analyzing spatial differences and relationships between land surface temperatures [4]. Thermal image sequences of water surface have been analyzed to measure the spatio-temporal flow velocity by studying the thermal features from the images [5]. However, thermal images have also been used in detecting foreign bodies in food [6]. However, in this study we presented a novel approach to detect impurities in water samples using thermal images.

III. Overall Framework

We use a sequence of thermal images of different water samples from its hot temperature to room temperature for detecting different impurities in it. We extract features from the series of thermal images for each of the samples. Our overall framework is showed in figure 1. There are three main modules in the framework. In the first data pre-processing module, the temperature of water surfaces are extracted using image processing techniques and temperature conversion algorithm. Then we transform the data into the subsequences of thermal images for our model input. We also label the images based on the impurity types and sources at this step. In feature extraction module, all the subsequences are passed into the

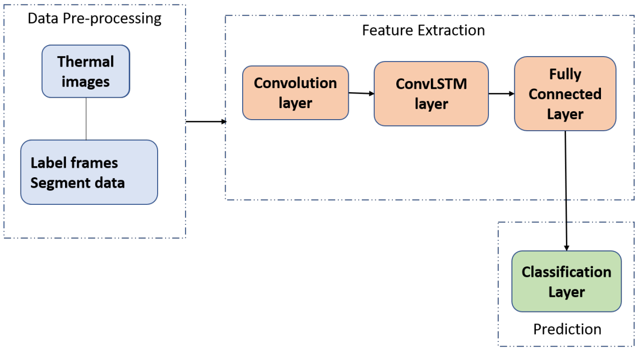

Fig. 1: Overall Framework

subsequent time-distributed convolution layers which extracts local spatial features of the individual images. We apply layer normalization [20] at the end of each convolution operations. Then ConvLSTM layers are stacked on top of time-distributed convolution layers to extract spatio-temporal features among the image subsequences. ConvLSTM combines all the gates of LSTM with 2D convolution and preserves hidden states between time steps. A fully connected dense layer is applied on the time distributed flattened features obtained from the last ConvLSTM layer and a supervised classification layer i.e., softmax layer categorizes the types of impurities added with the water samples. Later, we compute the distance of all water samples with safe water sample using discretized representation of feature vectors with Symbolic aggregated Approximation (SAX) [22].

IV. Proposed Framework

In this section, we present our proposed framework for determining the type of impurities in the water samples. In the following subsections, we describe each step of the framework in detail.

A. Data Pre-processing

We collected consecutive thermal images for each of the water samples using our developed android application for FLIROne thermal camera. In data pre-processing step, we processed the collected thermal images in three steps - i) Water surface extraction, ii) Temperature Extraction, iii) Prepare for feature extraction. In the first step, we extracted water surface area from the thermal image and cropped out the rest of the portions from the thermal images. This step helps us to focus only on the temperature of water surface ignoring other parts that comes into the image capture. In temperature extraction step, we extracted temperature value for each pixels of the interested region in the images. Infrared thermal images provide the radiation in the long-infrared range of the electromagnetic spectrum. However, we extract radiation data from the metadata of infrared thermal images and converted radiation values into estimated temperatures using standard thermography equations with the help of a R library named as 'Thermimage' [15]. In the last step, we transformed the images into a list of sub-sequences of temperature matrices to pass into the model .

B. Feature Extraction Model

In order to learn features from the prepared temporal sequences of temperature matrices, we developed a deep network with the combination of convolution and recurrent neural network. This network constructs the latent representation of our temporal sequences of temperature matrices. We use two layers of convolution operations to find the local translation invariant patterns of each of the images in the sequence in a hierarchical manner. Later, we apply ConvLSTM to capture better spatio-temporal features among given temporal sequences of temperature matrices. Convolutional LSTM (ConvLSTM) is introduced in [16] with the combination of CNN and LSTM where convolution structures are applied both at the input-to-state transition and state-to-state transition. It differs from the sequential CNN-LSTM network in which CNN layer is followed by LSTM layer. In the following subsections we describe the operations in different layers:

1) Convolutional Operation: The convolutional layer usually contains multiple convolution kernels or multiple filters to extract various types of features. For the implementation of k number of kernels, we obtain k feature matrices. The convolution operation can be expressed as follows:

$$Z_k = f(W_k * X + b) \tag{1}$$

where X is the input data, W_k is the $k-$th convolutional kernel and b denotes the offset. $*$ denotes the convolution operation.

2) Layer Normalization: Layer normalization is introduced in [20] which normalizes all the features to the neurons in a layer. It computes normalization statistics (i.e., mean and variance) across each features and does not depend on each other. We use layer normalization as it works effectively for recurrent neural networks and reduces the training time. For recurrent networks, it computes normalization statistics separately for each time steps. Mathematically, equations for layer normalization are given below:

$$\mu_j = \frac{1}{m}\sum_{i=1}^{m} x_{ji}; \quad \sigma_j^2 = \frac{1}{m}\sum_{i=1}^{m}(x_{ji}-\mu_j)^2; \quad \hat{x}_{ji} = \frac{(x_{ji}-\mu_j)}{\sigma_j^2} \tag{2}$$

Here, x_{ji} is the j-th feature in i-th hidden unit, m is number of hidden units in a layer, μ_j and σ_j^2 are the mean and variance for feature j, respectively, and $\hat{x}_{ji}$ is the normalized feature over all the hidden units in the layer.

3) ConvLSTM operation: ConvLSTM uses convolution operation with the given kernel instead of matrix multiplication among the gates of LSTM. This convolution operation of ConvLSTM reduces the model parameters and prevent overfitting. LSTM and ConvLSTM structure are showed in figure 2. Mathematically the updating procedure of ConvLSTM can be formulated as follows:

$$i_t^{conv} = \sigma(W_{xi}^{conv} * X_t + W_{hi}^{conv} * H_{t-1}^{conv} + b_i^{conv}) \tag{3}$$

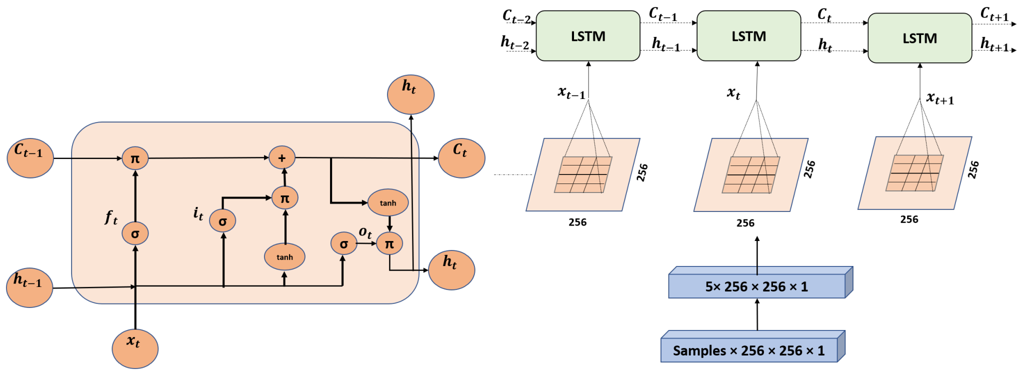

(a) LSTM (b) ConvLSTM

Fig. 2: (a) Basic LSTM cell, (b) Structure of ConvLSTM

$$f_t^{conv} = \sigma(W_{xf}^{conv} * X_t + W_{hf}^{conv} * H_{t-1}^{conv} + b_f^{conv}) \tag{4}$$

$$C_t^{conv} = f_t \odot C_{t-1}^{conv} + i_t \odot tanh(W_{xc} * X_t + W_{hc} * H_{t-1}^{conv} + b_c^{conv}) \tag{5}$$

$$o_t^{conv} = \sigma(W_{xo}^{conv} * X_t + W_{ho}^{conv} * H_{t-1}^{conv} + b_o^{conv}) \tag{6}$$

$$H_t^{conv} = o_t^{conv} \odot tanh(C_t^{conv}) \tag{7}$$

where $*$ denotes convolutional operation and $\odot$ denotes element-wise product; σ and $tanh$ are logistic sigmoid function and hyperbolic tangent function, respectively; W^{conv} and b^{conv} denote weights and biases learning from the training model. Here, the input data X_t, the output spatio temporal hidden state H_t^{conv}, the input gate i_t^{conv}, forget gate f_t^{conv}, cell state C_t^{conv}, and output gate o_t^{conv}, all are three dimensional matrices where the first two dimensions are spatio-temporal information and the third dimension is the number of convolutional filters.

Assume we have a set of temperature images $I = i_1, i_2, i_3, \cdots, i_N$, where i_t is the temperature image at timestamp t and N is the number of total images. Each of the images are 2D matrix of single channel. Each temperature image has a target categorical value Y which is the type of impurity in the water sample. However, we divide I into L local subsequences. Each subsequence is denoted as $S_{Ti} = x_{Ti}^1, x_{Ti}^2, \cdots, x_{Ti}^l$ where l is the length of each subsequence. After preparing the image subsequences, two dimensional convolution layer is applied to extract features for each of the images in the subsequence. Local feature extraction processes are performed independently with each other for each of the L sequences using "TimeDistributed" wrapper. With TimeDistributed wrapper, same structure of local feature extractors is applied for different time steps. We assume a sample input subsequence $S_{Ti} = x_{Ti}^1, x_{Ti}^2, \cdots, x_{Ti}^l$, which is a 4D tensor of $(l \times I_H \times I_W \times 1)$ format. The local feature extractor consists of two time-distributed local convolution layers. There are two types of features embedded in the sequences of temperature matrices, that is, spatial features in temperature matrices for different water samples and temporal features among consecutive temperature matrices. We apply convolution operation to each frame x_{Ti}^j (where $j \leq l$) simultaneously using time-distributed wrapper. In the first local convolution layer, two dimensional kernels with c number of filters are applied with convolutional stride $(2, 2)$ to extract features inside a temperature matrix using non-linear activation functions. The first convolution layer returns features with reduced shape, (n, l, I_h, I_w, c), which is thereafter served as the input to the next time distributed convolution layer. In the second local convolution layer, another 2D kernels are adopted with same convolutional stride to learn more general features in the temperature matrices and returns more reduced shape of features Ls_{Ti} for sequence S_{Ti}.

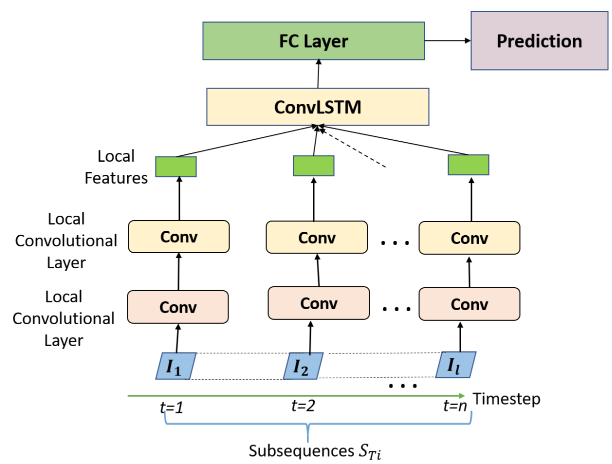

Fig. 3: Framework of the proposed model

We apply layer normalization after each convolution layer to normalize the features over all the hidden units of the layer. Later, a ConvLSTM layer with 2D kernels are adopted to learn deeper and sparser spatiotemporal features among the temporal sequences. The spatiotemporal features at each subsequence are flattened turning into shape $(n \times l \times l_3)$ where l_3 is the shape of flattened features. The framework of our proposed model is briefly presented in figure 3.

4) Classification Operation: At last, the feature vector is passed into another fully-connected layer with m units and a classification layer. The model is briefly presented in algorithm 1. As the target variable Y are discrete labels i.e., impurity types, the supervised learning layer applies a softmax layer, which is defined as follows:

$$P(y=m) = \frac{e^{v\theta_j^T}}{\sum_{k=1}^{K} e^{v\theta_j^T}} \tag{8}$$

Algorithm 1 Feature Extraction with ConvLSTM

procedure FEATURE EXTRACTION (**Input:** Training data I, **Output:** Predicted labels $Y'_{T1}, Y'_{T2}, \cdots, Y'_{TL}$)
  $S \leftarrow$ Divide I into L subsequences $S_{T1}, S_{T2}, \cdots, S_{TL}$
  for `each` S_{Ti} `in` S **do**:
    $Ls_{Ti} \leftarrow$ Local spatial features with convolution for each x^j_{Ti} in S_{Ti}
  end for
  Apply ConvLSTM on Ls_{Ti}'s from L subsequences
  Flatten features for each subsequence
  Apply dense layer on the flattened features
  $Y'_{T1}, Y'_{T2}, \cdots, Y'_{TN} \leftarrow$ Softmax on feature vectors
  return $Y'_{T1}, Y'_{T2}, \cdots, Y'_{TL}$
end procedure

To detect the quality of water samples, we measure the distance between each water sample and the fresh or safe water sample. We used SAX for discrete representation of feature vectors obtained from the fully connected layer. SAX divides the feature vectors using Piecewise Aggregation Approximation (PAA) and assign symbols to the PAA segments. The feature vectors are represented with a sequence of symbols. The final distance is defined as the total number of difference in the symbol sequence between any two feature vectors.

V. Experimental Results

In this section, we present the experimental results in detecting impurities and differentiating water sources using our framework.

A. Data Pre-processing

We prepared 25 water samples from 16 water sources with mixing other impurities i.e., salt, pencil lead powder, toothpaste etc. We tested some samples as it was collected from the source. With few water samples, a $10L$ water solution were prepared by mixing $20-100$ mg of impurities and we took $1L$ solution for our experiments. However, we collected water samples not only from the sources used for drinking and other activities, but also from the sources (i.e., ponds, rivers etc.) which are generally not used for drinking. Each water samples was tested with paper testing strips which gives us the ground truth of water properties. The paper testing strips provides various properties of water samples such as free chlorine, iron, copper, lead, nitrate, nitrite, bromine, total chlorine, fluoride, cyanuric acid, carbonate, total alkaline and pH level. Each of the samples collected from the known drinking sources are free of bromine, total chlorine and fluoride. We collected thermal images for each of the 25 samples. We heated the water samples to reach up to $100°C$ and captured thermal images until the water surface temperature reduces to room temperature. Here for this experiment, we maintained the room temperature as approximately $75°F$. For thermal image capture, we used FLIROne thermal camera which can be associated with an android smart phone. We developed an android app for FLIROne android camera to capture consecutive images with a certain time interval (i.e., 10 sec).

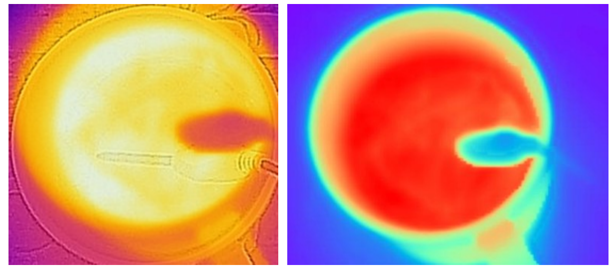

(a) Thermal image (b) Extracted temperature image

Fig. 4: Temperature image of thermal image

We extracted temperature and visual images for all the collected thermal images using a R package named as 'Thermimage' [15]. Extracted temperature image is showed in figure 4(b) for original thermal image in figure 4(a). Original pixel values in pre-allocated matrix of the same dimensions of the thermal image, are integers values which are radiance values or absorbed infrared energy values in arbitrary units. Calibration constants are used to fix the arbitrary unit problem in temperature conversion algorithm. Besides, the conversion algorithm includes Plank's law and the Stephan Boltzmann relationship, as well as atmospheric absorption, camera IR absorption, emissivity and distance.

Our collected thermal images, capture other portions including the water surfaces. Therefore, we extracted only water surface area from the images. To extract water surface area, we first obtained grayscale image of the original thermal image and applied Otsu's threshold to get a binary image. A circular shape like the upper surface of the water container was used as the kernel for morphological closing transformation. We isolated the contours using the expected contour area and prepare the mask by placing the minimum enclosing circle onto it. We cropped out the bounding rectangle ROI on the mask and considered temperature values only from the extracted water surface area. Figure 5 shows an example of captured thermal image and temperature image of extracted water surface.

However, the bounding rectangle of the water surface area are not of same size for all the images. Therefore, we center cropped the portion with size 256×256 from temperature matrices of water surface images. Later, we transformed the list of temperature matrices from all images into $Samples \times$

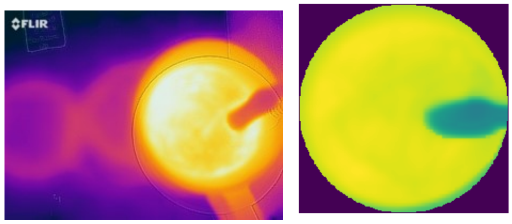

(a) original thermal image (b) extracted water surface

Fig. 5: Pre-processing of original thermal images

TABLE I: Parameters of the proposed model used in water impurity detection

No	Layer Type	Kernel	Stride	Activation
1	Local Convolution	(3,3)	(2,2)	LeakyReLu
2	ConvLSTM	(3,3)	(2,2)	LeakyReLu
3	FC Layer	256	-	Relu
4	Classification Layer	4	-	Softmax

$Timesteps \times Imageheight \times Imagewidth \times 1$ form for passing through our model. We separately prepared sub-sequences of 5 temperature matrices for each of the water samples and labeled them according to the category of impurities we added. It refers to that we are considering 50 seconds temperature changes for each pass in our model.

B. Model Settings

Our proposed feature learning algorithm based on ConvLSTM model were tested on the collected temporal sequences of thermal images from different water samples. The parameters in different layers are listed in Table I. We adopted categorical cross-entropy as the loss function and stochastic gradient descent for optimizing the loss of the model. In our developed model, the kernel, stride and filter number of two convolution layers are set to [(3,3), (2,2), 128] and [(3,3), (2,2), 64], respectively.

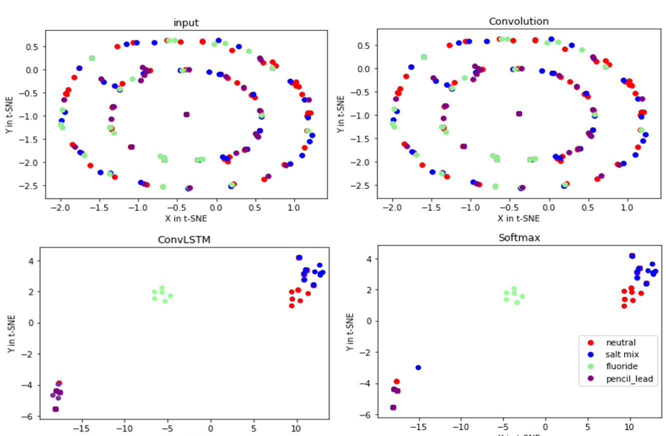

Fig. 6: Visualizing features from ConvLSTM model at different layers

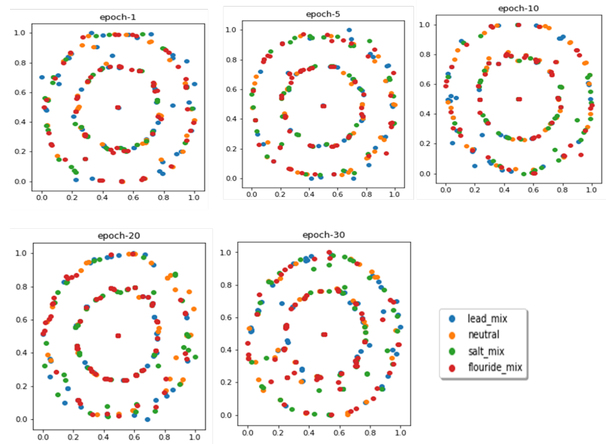

Fig. 7: Visualizing features from LSTM model

We visualized the features for different kind of water samples in different layers of ConvLSTM model in figure 6(a). This feature visualization helps us to understand the process of differentiating the categories of impurities over different layers in the model. Here, we used t-SNE method [21] to show the features extracted by each layers in our proposed model. T-SNE maps the high dimensional data from high dimensional space to two-dimensional space. The feature maps from input data, the local convolutional layer, ConvLSTM layer and the last softmax layer are showed in figure 6. The features of water samples with different impurities can be distinguished by different colors in the figure. It is obvious from the figure that the more the layers get deep, the features get more separated. At the initial stage in the raw input data, the features of all four impurities are all combined together. After the local convolutional layers, features are still dispersed and combined together. However, starting from ConvLSTM layer, the features from same mixture types begin to be placed together. At ConvLSTM layer, most of the features from the fluoride and the salt mix type water sample, clustered together, while the neutral type are still mixed together with lead mix and salt mix. The fully connected layer further separates the features of the four mix types and the features of the same mix type are placed closer than before. At the last layer, there exists some sparse feature vectors which are not completely separated. In comparison with the proposed algorithm, we presented feature evolution at different epochs during training using stacked LSTM network in figure 7. For this network, we took the mean temperature from each temperature images of water samples and prepare a temperature sequence. The figure shows stacked LSTM network with only temperature sequence from different samples cannot differentiate features for these four categories of mixtures dissolved in water. We also experimented with LSTM layer by replacing ConvLSTM layer in our proposed model which also acts same as satacked LSTM network. Table II shows the average accuracy for predicting each category of impurities of different amount with classification using our proposed model.

TABLE II: Accuracy of detecting different category of water samples

Added material	Amount(mg)	Accuracy(%)
Salt	20	70.3
Salt	50	80.2
Salt	100	82.4
Fluoride	20	65.2
Fluoride	30	69.4
Fluoride	50	72.9
Pencil lead powder	20	67.5
Pencil lead powder	30	70.1
Pencil lead powder	40	73.4

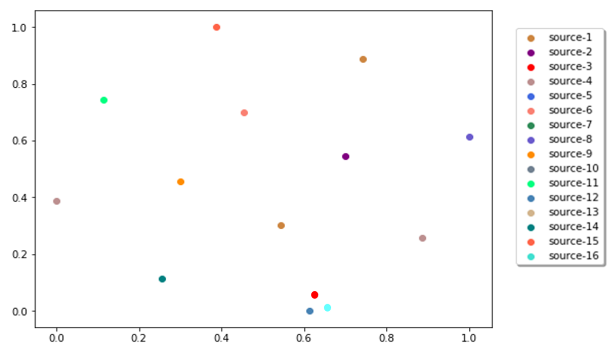

Fig. 8: Feature space for differentiating water-sources

It is obvious from the accuracy results that with the increment of impurity amount, the model can predict the impurity category more accurately. However, for salt mixed water sample, the model performs better even for small amount. However, we also differentiated water samples based on the sources. Figure 8 shows features for each of the water sources with t-sne plot. Although most of the water sources are safe for drinking as no harmful substances are present above standard amount, they are quite distant in the feature space. The paper tester provides different amount of hardness, carbonate, alkaline, free chlorine and pH level. However, water samples from source 3, 12 and 16 are closer in feature space than that of other samples. Those samples were collected from a hilly area and the hardness, alkaline and pH level were high in amount. The sources located in the middle of the feature space are of similar pH level but differs in other properties of water i.e. amount of carbonate, iron, cyanuric acid, hardness and alkaline.

C. *Differentiating Mix types*

We converted our features vectors into discretized representation with SAX. In Table III, we presented the average SAX distances between each category of water samples and drinking water samples. It shows that features from lead mix and fluoride mix water are more distant than the salt mix water sample with fresh water sample.

TABLE III: SAX distance of all mix types from safe water

Mix type	Distance
Salt	3.35
Fluoride	6.7
Lead	4.69

VI. Limitations and Future work

Our work in this study is a preliminary step to investigate the feasibility of using thermal images to determine the water quality. There are some limitations of our work due to lack of resources and lab settings. We collected water samples from different residential areas in USA and prepared some samples with three kinds of impurities. For this study, we used considerably large amount of impurities compared to the actual permitted amount of impurity. For example, we used 20-40mg of lead powder to prepare 10L solution for our experiments while permissible lead amount in water sources is approximately 0.015mg/L which is 100 times smaller than the amount we considered. The measuring scale for such precise amount is very expensive. Besides, some minerals i.e., lead, arsenic etc., are very scarce in salt form in the market. We conducted experiments with best possible settings in residential home considering these limitations. We experimented the variation of thermal characteristics due to the use of impurities in water. Our framework is useful to compare the quality of an unknown water sample with the known safe water sample. We captured thermal images in 10 seconds interval as we observed hot water samples take at least 10–15 minutes to reach to room temperature. Due to thermal inertia and higher thermal heat capacity, water stores heat well. Therefore, we chose not to select higher time interval for longitudinal image capture.

As future study, we might extend this work to investigate the presence of smaller amount of impurities in water samples. For testing and detecting the amount of other minerals, we can build machine learning based model involving chemical sensors along with the thermal properties of water samples to detect the noticeable minerals in water.

VII. Conclusion

In this work, we experimented with water samples that are mixed with different impurities in different amounts. We used the thermal property of water samples to identify the materials. For feature extraction from the temperature matrices of thermal images, we used ConvLSTM based network. We visualized how this model differentiates feature vectors for different type of water samples. Finally, we also scored each water sample using discrete representation of their feature vectors. Given more time and resources, we could extend this project for creating more artificial samples with smaller amount of impurities and testing on originally contaminated water samples. This work is considered to be the initial step for using machine learning to analyze thermal images for water quality assessment.

VIII. ACKNOWLEDGMENT

This work is partially supported by NSF CNS grant 1544687 and NSF CNS grant 1640625.

REFERENCES

[1] A. Gupta and E. Ruebush, "Aquasight: Automatic water impurity detection utilizing convolutional neural networks," *arXiv preprint arXiv:1907.07573*, 2019.

[2] H. Fernandez-Canque, B. Beggs, E. Smith, T. Boutaleb, H. Smith, and S. Hintea, "Micro-organisms detection in drinking water using image processing," *cell*, vol. 15, pp. 4–2, 2006.

[3] J. Wahid and Q. Ahsan, "Detection of impurities in water by measuring capacitance," in *8th International Conference on Electrical and Computer Engineering*, pp. 88–91, IEEE, 2014.

[4] W. Kuang, Y. Liu, Y. Dou, W. Chi, G. Chen, C. Gao, T. Yang, J. Liu, and R. Zhang, "What are hot and what are not in an urban landscape: quantifying and explaining the land surface temperature pattern in beijing, china," *Landscape ecology*, vol. 30, no. 2, pp. 357–373, 2015.

[5] D. Lin, A. Eltner, H. Sardemann, and H.-G. Maas, "Automatic spatio-temporal flow velocity measurement in small rivers using thermal image sequences.," *ISPRS Annals of Photogrammetry, Remote Sensing & Spatial Information Sciences*, vol. 4, no. 2, 2018.

[6] G. Ginesu, D. D. Giusto, V. Margner, and P. Meinlschmidt, "Detection of foreign bodies in food by thermal image processing," *IEEE Transactions on Industrial Electronics*, vol. 51, no. 2, pp. 480–490, 2004.

[7] D. A. Stonestrom and J. Constantz, *Heat as a tool for studying the movement of ground water near streams*. No. 1260, US Dept. of the Interior, US Geological Survey, 2003.

[8] A. Chojnacki, C. Dai, A. Farahi, G. Shi, J. Webb, D. T. Zhang, J. Abernethy, and E. Schwartz, "A data science approach to understanding residential water contamination in flint," in *Proceedings of the 23rd ACM SIGKDD International Conference on Knowledge Discovery and Data Mining*, pp. 1407–1416, ACM, 2017.

[9] A. Shkurin *et al.*, "Water quality analysis using machine learning algorithms," 2016.

[10] "Safe drinking water act (sdwa) — us epa." https://www.epa.gov/sdwa. Accessed: 2020-01-20.

[11] "Cities with the worst tap water in us - business insider." https://www.businessinsider.com/cities-worst-tap-water-us-2019-3. Accessed: 2020-01-20.

[12] M. Allaire, H. Wu, and U. Lall, "National trends in drinking water quality violations," *Proceedings of the National Academy of Sciences*, vol. 115, no. 9, pp. 2078–2083, 2018.

[13] "Get the lead out@ONLINE." https://marylandpirg.org/sites/pirg/files/reports/MDE-GetTheLeadOut-20Mar19.pdf. Accessed: 2020-01-20.

[14] "Report: Up to 110 million americans could have pfas-contaminated drinking water." https://www.ewg.org/research/report-110-million-americans-could-have-pfas-contaminated-drinking-water.WwgkkC-ZPBJ. Accessed: 2020-01-20.

[15] G. Tattersall, "Thermimage: Thermal image analysis," 2017.

[16] S. Xingjian, Z. Chen, H. Wang, D.-Y. Yeung, W.-K. Wong, and W.-c. Woo, "Convolutional lstm network: A machine learning approach for precipitation nowcasting," in *Advances in neural information processing systems*, pp. 802–810, 2015.

[17] F. Xiong, X. Shi, and D.-Y. Yeung, "Spatiotemporal modeling for crowd counting in videos," in *Proceedings of the IEEE International Conference on Computer Vision*, pp. 5151–5159, 2017.

[18] Z. Qiu, T. Yao, and T. Mei, "Learning deep spatio-temporal dependence for semantic video segmentation," *IEEE Transactions on Multimedia*, vol. 20, no. 4, pp. 939–949, 2017.

[19] H. Qiao, T. Wang, P. Wang, S. Qiao, and L. Zhang, "A time-distributed spatiotemporal feature learning method for machine health monitoring with multi-sensor time series," *Sensors*, vol. 18, no. 9, p. 2932, 2018.

[20] J. L. Ba, J. R. Kiros, and G. E. Hinton, "Layer normalization," *arXiv preprint arXiv:1607.06450*, 2016.

[21] L. v. d. Maaten and G. Hinton, "Visualizing data using t-sne," *Journal of machine learning research*, vol. 9, no. Nov, pp. 2579–2605, 2008.

[22] E. Keogh, K. Chakrabarti, M. Pazzani, and S. Mehrotra, "Dimensionality reduction for fast similarity search in large time series databases," *Knowledge and information Systems*, vol. 3, no. 3, pp. 263–286, 2001.